72nd International Astronautical Congress (IAC), Dubai, United Arab Emirates, 25-29 October 2021.

IAC-21-C1.1.12

Formation Flying Control of the Relative Trajectory Shape and Size Using Lorenz Forces

Goncalo Amaro[a], Danil Ivanov[b]*, Anna Guerman[c]

[a] *University Beira Interior, Covilha, Portugal,* amaro.space21@gmail.com
[b] *C-MAST Center for Mechanical and Aerospace Science and Technology, University Beira Interior, Covilha, Portugal,* danilivanovs@gmail.com
[c] *C-MAST Center for Mechanical and Aerospace Science and Technology, University Beira Interior, Covilha, Portugal,* anna@ubi.pt

* Corresponding Author

Abstract

A formation flying control algorithm using the Lorentz-force for Low-Earth Orbits to achieve a trajectory with required shape and size is proposed in the paper. The Lorentz force is produced as the result of interaction between the Earth's magnetic field and an electrically charged spacecraft. Achieving the required trajectories represents a challenge since the control is the variation of the satellite's charge value. A Lyapunov-based control function is developed for elimination of the initial relative drift after launch; it aims at reaching a required relative trajectory with pre-defined shape and size. The Lyapunov-based control algorithm is constructed to correct different parameters of the relative trajectory at different relative positions. The required amplitudes for close relative trajectories for in-plane and out-of-plane motion as well as the relative drift and shift of elliptical orbits are controllable using this Lorentz force algorithm. Due to the absence of full controllability, the algorithm is incapable to correct all the parameters of the relative trajectory. The proposed control allows to converge to the trajectory with required shape and size, though with some oscillating errors in the vicinity of the required trajectory parameters. Numerical simulation of the relative motion is used to study performance of the control algorithm for three cases – one controlled satellite, two controlled satellite and five satellites. It implements the model of the geomagnetic field as a co-rotating tilted dipole. The convergence time and final trajectory accuracy are evaluated for different algorithms and satellite parameters.

Keywords: formation flying, Lorenz force, Lyapunov-based control algorithm

1. Introduction

A satellite flying formation is defined as a set of satellites moving in close relative trajectories that can control their relative position and/or relative velocities, keeping close distances and solving a common problem.

A charged particle, whose moving with a determined velocity relative to the Earth's magnetic field, accelerates in a direction perpendicular to its velocity vector and the local magnetic field vector due to the Lorentz force [1]. The application of this force for a spacecraft formation flying control is a relatively new idea and, therefore a rather unstudied one. The first works about the Lorentz force effects on charged bodies were conducted by Schaffer and Burns who developed a model explaining the influence of the plasma environment on the dynamics of charged dust particles orbiting Jupiter and Saturn [2]. These studies proved that the orbital motion and dynamics are greatly influenced by the Lorentz force and that this magnetic force along with gravity effects, lunar perturbations, and solar pressure are responsible for the existence of gaps in either Jupiter's and Saturn's ring resonances. These works represented a valuable contribution to validating models concerning the charging of particles and the demonstration that Lorentz force effects lead to non-Keplerian orbits.

Following the work developed by Schaffer and Burns, Peck conducted a series of studies proposing the implementation of the Lorentz force for the development of a propellantless satellite technology. In paper [1] Peck explores the development of Lorentz Augmented Orbit (LAO) system which could be capable of using this effect for orbital control. It also provides a wide range of LAO systems that would be solutions for Earth escaping, drag compensation, formation flying control, inclination control, nodal precision control, new sun synchronous and even non-Keplerian polar orbits. This Lorentz force effect is experienced individually by any charged spacecraft and, in contrast to Coulomb force, it in not resultant from the interaction between two charged spacecraft. Instead, this force is caused by a magnetic interaction between the

charged spacecraft's relative velocity and the environments magnetic field. Both the direction and magnitude of the Lorentz force are a function of the satellite's orbital motion (presenting different values for different orbital positions and therefore being sensible to the orbits geometry), being its direction always perpendicular to the spacecraft's velocity and the local magnetic field vector. Peck [1] also presents a possible design for LAO system configurations. Although LAO system configurations does not involve the use of electrodynamic tethers, the operation physics of both devices are similar. For a LAO spacecraft, the body acts as a point charge which moves with a velocity of thousands of meters per second relatively to the planet magnetic field. The moving charge represents the current similar to the one acting in electrodynamic tethers [3].

LAO equipped spacecraft formations are not designed to control their motion via attractive or repulsive forces, in contrast to the systems described in [4] and [5] papers. In the paper [5] the authors examine the possibilities the Electromagnetic Formation Flying systems (EMFF) for nearby satellites inspection possibilities. These inspections would be performed by a group of three satellites, each one capable of controlling both their attitude and relative position, individually, inside the formation by driving a current through a set of three magnetic coils. Thus, the formation motion control is performed by this magnetic dipole creation enabling the relative state control of each formation element. This magnetic interaction offers increased control, guidance, and navigation capabilities. Another study that focused on the replacing of large fuel based systems by embracing a formation flying scheme is [4]. This study gives an alternative technology for NASA's Terrestrial Planet Finder (TPF) mission, based on the application of a multiple spacecraft with electromagnetic control capabilities. Focusing on the elimination of secondary effects associated with propellant based systems, such as fuel depletion, optical contamination, or plume impingement, the authors develop an optimized electromagnetic system capable of replacing the more traditional fuel-based control options. The application of electromagnetic forces, such as the Lorentz force, enables systems like TPF to control the relative translational motion and attitude, as well as the inertial rotation of the formation. As the authors concluded, EMFF system concepts represent the most attractive options for this type of mission, especially when long mission lifetimes are considered (in theory, the proposed EMFF system is able to operate indefinitely, or at least until the component failure). A characteristic that when allied with the propellantless possibilities reinforces the viability of EMFF mission concepts.

Another major aspect to account when developing a LAO system, namely during the simulation of the system operation is the Earth's tilted magnetic dipole feature. This Earth magnetic model is widely used in numerous studies involving the implementation of Lorentz control systems, including the study [6]. This paper goal is to examine the application of the Lorentz force as the mean orbital maneuvering control of a charged spacecraft, but also to demonstrate the utilization of such electromagnetic forces for the construction and reconfiguration of formation flying configurations. By studying and comparing the formation flying control considering a tilted and a nontilted dipole model, the authors conclude that without considering the tilted dipole feature it is not possible to use the Lorentz force as a mean for the formation motion control. Due to the geometric interaction between magnetic field and velocity vectors, the dipole's rotation axis inclination feature, even if small, allows the control of the satellites relative motion in contrast to a situation where this feature is nonexistent. Thus, as proved by the simulation results in [6], the adoption of a tilted dipole model is a crucial step to obtain reliable and adequate results when simulating LAO systems.

The Lorentz electromagnetic force has been widely studied for several applications, not only considering the formation flying control but also a set of satellite control problems, as in the case of [7] where the authors propose a Lorentz based control scheme for the attitude control of a spacecraft in LEO. In this paper, the authors goal is the development of a pitch and roll direction torques electromagnetic controller that could replace the traditional attitude control systems. However, the authors were forced to consider a elliptical orbit as a way of introducing a varying relative motion between the satellite and the Earth's magnetosphere, once a nontilted dipole model was considered during the simulations [7]. Another example of a LAO controlled spacecraft development is the paper [8] case, presenting the development of a new propellantless orbital control system. By executing two different time varying studies, considering one day averaged and single orbit averaged approaches, the authors realise that after a 24 hour period a corrector must be applied to counter both J2 and Lorentz influence on three of the six classical orbit elements. To perform these studies, a new model that bounds a Lorentz augmented orbit with a J2invariant perturbations models is successfully developed and simulated [8]. The orbital transfer case and the orbital maneuvering for single satellites as well as for satellite formations is also studied in [9], [10] and [6]. While opting for the development of a hybrid system (a Lorentz acceleration system allied with a thruster generated system) and a nonlinear dynamical model scheme for the maneuver control [6], the authors

proposed new control schemes that proved to be effective. The positive results were obtained not only for elliptical orbits cases but also for alternative Lorentz augmented relative orbital situations. This control scheme adaptive profile is also considered in the [10] study case, where the developed algorithm for a formation control situation is successfully applied for an orbital transfer.

The purpose of the paper is to develop Lypunov-based control algorithm using Lorenz force only in order to achieve the required trajectory of the defined size and shape. The phase angles of the in-plane and out-of-plane motion remained uncontrolled. The structure of the rest of the paper is as follows. In Section 2 a problem statement is formulated, the motion equations are presented. In Section 3 the control algorithm is derived and its impelemtation using Lorenz force is described. In Section 4 the proposed algorithm is applied for a set of problems for formation flying consisting of two satellites and 5 satellites. In the last Section the results of the work are summarized.

2. Problem Statement

The problem statement of this work is as follows. Several satellites equipped with charging capable devices are considered to be in LEO. The Earth magnetic field is modelled as the tilted dipole model previously described in Chapter 3. The satellites are considered to be point masses, whose attitude motion is not considered throughout the work. Due to the influence of the Debye shielding in LEO orbits, intersatellite and Earth satellite electrostatic interaction is neglected. For simulation of controlled motion, the second harmonic of the geopotential J2 is taken into account as the only environmental perturbation. Once the satellites are considered to be point masses equipped with charging capable devices, there is no full controllability of the translational relative motion. Thus, the objectives of the control algorithm are to eliminate the formation relative drift, to achieve the required value for the relative shift as well as out-of-plane and in-plane relative trajectory amplitudes. The phase angles for the in-plane and out- of-plane relative motion remain uncontrolled. To achieve this goal, a Lyapunov based control algorithm is developed.

It is also necessary to study the performance of the developed algorithm depending on a large variety of factors, such as charging capacity maximum value, orbital height, and the variation of the initial conditions. Through Monte Carlo simulations method is used to evaluate the influence of these parameters on the convergence time or the accuracy of the control algorithm.

2.1 Motion equations

The relative motion of two arbitrary satellites in formation can be described by the linear approximation equations named after the Hill-Clohessy-Wiltshire (HCW) [11]. Taking the Hill reference frame as in, Fig.1, the HCW model offers an analytic solution for the free motion of two or more satellites in an orbital system with a origin moving along the circular orbit in the central gravitational field. HCW equations offer a linear approximation for the relative orbital motion, equations that otherwise would be too complex for the analytical solution. However, this model can only be used in situations where the intersatellite distance is much smaller than the reference orbital point radius [10]. Several assumptions are applied while solving these sets of equations, to simplify the derivation processes, hence affecting the accuracy of the results.

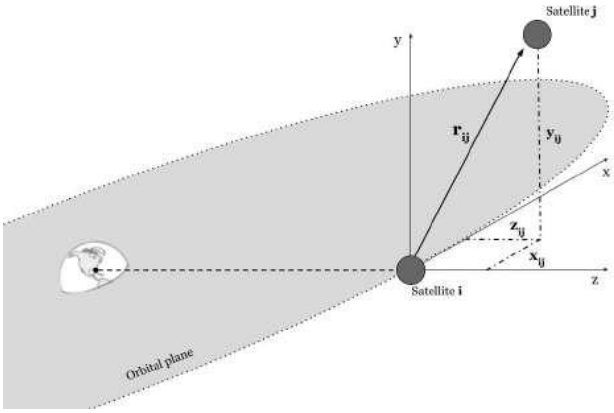

Fig. 1. LVLH reference frame

The Hill-Clohessy-Wiltshire equations are utilized to describe the relative motion of two arbitrarily chosen satellites within the swarm [12], in a leader-follower system expressed in the rotating Local-Vertical-Local-Horizontal reference frame (LVLH) designated as $Oxyz$. Its origin is located at a reference point moving along a circular orbit with radius r_0, at an orbital angular velocity ω. The *z*-axis points towards the radial direction, the *y*-axis is aligned with orbital momentum and the *x*-axis completes the right-handed orthogonal frame. These linearized ordinary differential equations of free motion can be solved analytically. A complete solution is the sum of the solution to the homogeneous equation, representing the effect of initial conditions, and a particular solution representing the effects of the applied forces, where the electromagnetic control force is considered. The equations are valid for small relative distances, therefore the relative distance between the leader and follower must be several orders of magnitude smaller than the orbital dimensions.

Let $\mathbf{r}_i = (x_i, y_i, z_i)$ and $\mathbf{r}_j = (x_j, y_j, z_j)$ be the vectors of the *i*-th and *j*-th satellites in the LVLH reference frame, $i \neq j, i = 1,..., N, j = 1,..., N,$ where N is the number of the satellites in the swarm. Then the components of the relative position vector $\mathbf{r}_{ij} = \mathbf{r}_j - \mathbf{r}_i = (x_{ij}, y_{ij}, z_{ij})$.

Consider the controlled motion equations of the swarm, and assume that each i-th satellite is equipped with a motion control system able to produce the acceleration $\mathbf{u}_i$. The relative motion of two i-th and j-th satellites in the LVLH reference frame are as follows:

$$\begin{aligned} \ddot{x}_{ij} + 2\omega\dot{z}_{ij} &= u_{ij}^x, \\ \ddot{y}_{ij} + \omega^2 y_{ij} &= u_{ij}^y, \\ \ddot{z}_{ij} - 2\omega\dot{x}_{ij} - 3\omega^2 z_{ij} &= u_{ij}^z, \end{aligned}$$

where $\mathbf{u}_{ij} = \mathbf{u}_j - \mathbf{u}_i = (u_x^{ij}, u_y^{ij}, u_z^{ij})$ is the difference of the two control accelerations written in LVLH frame. Its solution in case of $\mathbf{u}_{ij} = 0$ can be written as follows [13]:

$$\begin{aligned} x_{ij} &= 2B_2^{ij}\cos\left(\omega t + \psi_{ij}\right) + B_3^{ij}, \\ y_{ij} &= B_4^{ij}\cos\left(\omega t + \varphi_{ij}\right), \\ z_{ij} &= 2B_1^{ij} + B_2^{ij}\sin\left(\omega t + \psi_{ij}\right), \end{aligned}$$

where the parameters $B_1 - B_4, \psi, \varphi$ are the motion parameters. From the previous solutions it is possible to conclude that B_1 is the parameter describing the instant ellipse drift, B_3 the responsible for the ellipse center shift, while B_2 and B_4 describe the ellipse in-plane and out-of-plane motion amplitude, respectively. It can be considered as osculating elements changing under the control according to the following differential equations

$$\begin{aligned} \dot{B}_1^{ij} &= \frac{1}{\omega}u_{ij}^x, \\ \dot{B}_2^{ij} &= \frac{1}{\omega}\left(u_{ij}^z\cos\psi_{ij} - 2u_{ij}^x\sin\psi_{ij}\right), \\ \dot{B}_3^{ij} &= -3\omega C_{ij} - \frac{2}{\omega}u_{ij}^z, \\ \dot{B}_4^{ij} &= -\frac{1}{\omega}u_{ij}^y\sin\varphi_{ij}, \\ \dot{\psi}_{ij} &= -\frac{1}{\omega A}\left(u_{ij}^z\sin\psi_{ij} + 2u_{ij}^x\cos\psi_{ij}\right), \\ \dot{\varphi}_{ij} &= -\frac{1}{\omega B}u_{ij}^y\sin\varphi_{ij}. \end{aligned}$$

2.2 Lorenz force

This paper aims for the development of a viable propellantless formation flying control, thus, it is necessary to describe the technical aspects of the electromagnetic force used in this paper. Any charged particle, moving with a given velocity relative to a magnetic field, accelerates. This acceleration is directed along the normal vector of the plane formed by the velocity and magnetic field vectors. This effect is called the Lorentz force [35], [46]. This force is valid for any charge q with a relative velocity $\mathbf{v}$ in an electric and magnetic field, $\mathbf{E}$ and $\mathbf{B}$ respectively, and is given by

$$\mathbf{F}_L = q\left(\mathbf{v}\times\mathbf{B}\right).$$

Charged spacecraft orbiting the Earth are affected by this force too, however unlike the Coulomb force effects, the Lorentz force is not resultant from the interaction between two charged satellites [8], [14]. The Lorentz force case, is caused by the interaction between the spacecraft's velocity and the Earth's rotating magnetic field. Note that both direction and magnitude of the Lorentz force depend on the satellite orbital motion. These Lorentz force vector is depicted in the Fig. 2.

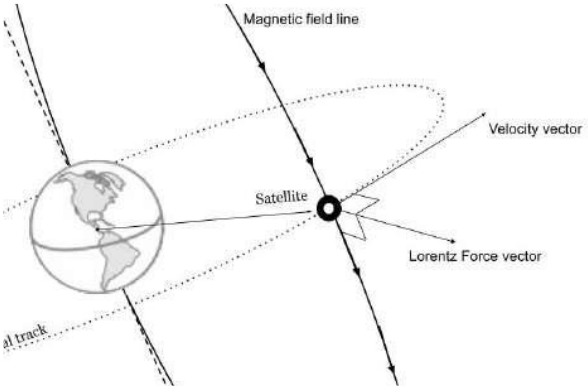

Fig. 2. Lorenz Force direction

Another important factor is related to the Debye shielding whose effects, depending on the orbit's altitude and geometry, may influence the orbiting charged satellite. Debye shielding is a concept responsible to quantify the response of the environment (in this case the plasma surrounding) to electrical fields when releasing charged particles. This effect is quantified through the Debye length, a measure of the electrostatic net effect of a charge carrier, and how far it persists. For the LEO the measured Debye length values are small (~= 1cm) , and the satellite velocities are much larger than the magnetic field rotational speed, which leads to the overlapping of the Lorentz force over

other electromagnetic forces such as the Coulomb force. Therefore, the existence of Debye shielding results in a functioning improvement in Lorentz capable spacecraft. The presence of this Debye effect enhances the charge storage capacity, hence enhancing LAO systems performance when in LEO [3]. With the rise of orbital altitude comes a Debye length increase, which combined with the lower spacecraft's relative velocity (to the magnetic field) results in the dominance of the Coulomb effects over the Lorentz force. Thus, at LEO, satellite formation control systems requiring Coulomb's attractive and repulsive force based devices are not as effective as the those based on the Lorentz force.

When considering LAO capable systems, there are some aspects relative to the system's morphology that should be accounted in the design phase. The first one is the maximization q/m, once the Lorentz force reveals to be proportional to the charge. However, the charge losses rate to the environment should be a major concern, once this rate will be directly linked to the power required for the control system functioning, thus the design's discharge susceptibility shall be closely examined. From studies such as [1] and [3], the best achieved design for a LAO spacecraft is with a surface of a conducting sphere, though this shape preludes charge concentrations that would otherwise encourage arcing and discharge into the plasma. To counter this phenomena, the authors propose the action of designing a surrounding conducting sphere, therefore establishing a Faraday cage that would completely protect the interior components from electrical discharge.

2.3 Dipole Geomagnetic Field Model

For the simulation of the Earth magnetosphere there are several models, with different precision values accordingly to the observation methods and to the correspondent period of measurements. Models like the International Geomagnetic Reference Field (IGRF), CHAOS7 or LCS1 are frequently used when a high degree of precision is needed in cases where the small variations of the Earth magnetic filed values could signify undesirable manifestations on the mission's objective [15].

However, due to their high precision magnetic field variation data, these models take a large numerical calculation steps, which in the case of this study would mean a more complex simulation stage. Therefore, a simpler generic model was adopted, the Tilted Dipole Geomagnetic Model Fig. 3 [8]. Despite being considered a "raw" simulation of the real Earth Geosphere, this is rather easy to implement computationally and, although providing low precision data, it matches the precision needed for this technology validation study.

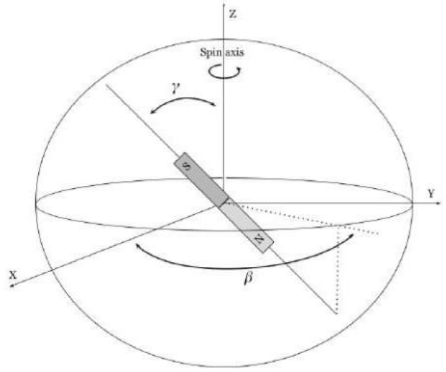

Fig. 3. Earth's geomagnetic model considered tilted dipole geomagnetic model

Considering the propositions stated above, and based on the electrodynamics classical theory, the Earth's magnetic model B and its Electric Field model E are defined as

$$\mathbf{B} = \frac{B_0}{r^3}\left[3\left(\hat{\mathbf{N}}\cdot\mathbf{R}_i\right)\mathbf{R}_i - \hat{\mathbf{N}}\right]$$

where Ri corresponds to the spacecraft position unit vector and r its magnitude, B0 is the Earth magnetic dipole moment with the value of B0 = 8 × 106(T km3), and the ˆN parameter defining the dipole's direction unit vector, which is not coincident with the Earth's rotation axis, and expressed as

$$\hat{\mathbf{N}} = \begin{bmatrix} \hat{N}_x \\ \hat{N}_y \\ \hat{N}_z \end{bmatrix} = \begin{bmatrix} \sin\gamma\cos\beta \\ \sin\gamma\sin\beta \\ \cos\gamma \end{bmatrix}$$

with γ = 10.26◦ as the angle measured between the magnetic and geocentric north pole, and $\beta = \beta_{G0} + \omega_e t$, where β_{G0} is the Greenwich's longitude and ω_e = 4.1667×10^{-3}(◦/s) is the Earth's angular rotation rate.

2. Control Algorithm

The proposed control algorithm aim is to control and maintain a satellite formation after the orbital deployment. The direct Lyapunov method is applied for the development of the control algorithm. This method provides the stability of a body's controlled motion [16]. Building the Lyapunov functions for a given automatic control system enables the estimation of the time and quality variation of the control. This method begins by defining an attraction region and, consequently, develops a state for the initial values. By giving a prevision of the area of the initial disturbance (which, over time, is not exceeded), this method provides a solution for the overcorrection problem [16].

The purpose of the control algorithm is to achieve the required B_i , i = 1, 2, 3, 4 parameters, the following parameters deviations are considered

$$\Delta B_2 = B_2 - B_2^{des},$$
$$\Delta B_3 = B_3 - B_3^{des},$$
$$\Delta B_4 = B_4 - B_4^{des},$$

where the relative orbit ellipse is defined by the Bides elements, with the des index defining the desired parameters, and the B_i representing the instantaneous parameter values measured along the orbit track. The implementation purpose of these equations is to allow the formation to maintain the required relative orbit shape. Important to remark that being the main goal of the present work the elimination of the drift, the difference between the instantaneous B_1 and the desired was not considered once it would result in a extra redundant step.

The relative orbit control is divided into two stages: a first one with the objective of eliminating the drift and achieving the desired ellipse shift; and then a second one where the desired in-plane and out-of-plane motion amplitudes are obtained.

3.1 Lyapunov-based control

In order to set the relative drift B_1 and the relative shift ΔB_3 to zero, the following Lyapunov function was developed for the first stage as in [13]:

$$V = \frac{1}{2}B_1^2 + \frac{1}{2}\Delta B_3^2.$$

Deriving the equation above with time, and substituting some of the terms for the simplifications result in the following:

$$\dot{V} = B_1 \dot{B}_1 + \Delta B_3 \Delta \dot{B}_3 = $$
$$= \frac{1}{\omega} B_1 u_x + \Delta B_3 \left(-3B_1\omega - \frac{2}{\omega} u_z \right).$$

In order to achieve $\dot{V} < 0$ and obtain the global asymptotic stability, when B_1 $B_1 = 0$ and $\Delta B_3 = 0$, is the following control should be applied

$$u_x = -k_a B_1, \ k_a > 0,$$
$$u_z = \frac{1}{2}\left(-3B_1\omega^2 + k_b \omega \Delta B_3\right), \ k_b > 0.$$

After reaching the desired values for B_1 and B_3 , inside the convergence zone, the algorithm starts a second stage, in order to achieve both the in-plane and out-of-plane required trajectory amplitude values. Thus, the following Lyapunov function used is

$$V = \frac{1}{2}B_1^2 + \frac{1}{2}\Delta B_2^2 + \frac{1}{2}\Delta B_3^2 + \frac{1}{2}\Delta B_4^2.$$

Its time derivative is the following

$$\dot{V} = -\frac{1}{\omega}\left(B_1 - 2\Delta B_2 \sin\psi\right)u_x + \frac{1}{\omega}\left(\Delta B_2 \cos\psi - 2\Delta B_3\right)u_z -$$
$$-3B_1\Delta B_3\omega - \frac{1}{\omega}\sin\varphi\Delta B_4 u_y.$$

Consider the following control vector:

$$u_x = k_x\left(B_1 - 2\Delta B_2 \sin\psi\right), \ k_x > 0,$$
$$u_y = k_y \Delta B_4 \sin\varphi, \ k_y > 0,$$
$$u_z = -k_z\left(\Delta B_2 \cos\psi - 2\Delta B_3\right), \ k_z > 0.$$

If this control is substituted into the derivative of Lyapunov function

$$\dot{V} = -\frac{k_x}{\omega}\left(B_1 - 2\Delta B_2 \sin\psi\right)^2 - \frac{k_y}{\omega}\left(\sin\varphi\Delta B_4\right)^2$$
$$-\frac{k_z}{\omega}\left(\Delta B_2 \cos\psi - 2\Delta B_3\right)^2 - 3B_1\Delta B_3\omega.$$

The term $-3B_1\Delta B_3\omega$ could not be negative, but after the first control stage its value will be much smaller than the sum of the first three terms in this equation. Therefore, it is assumed that this term takes a rather insignificant impact on the Lyapunov function derivative.

It should be noted that the calculated control may not be possible to implement considering the system's charging capacity limits. Henceforth, it is required to take into account the implementation restrictions during the controlled motion simulation. This important issue is addressed in the next section.

3.2 Control implementation using Lorenz-force

As referred to in the previous paragraph, it is now necessary to implement the calculated control. In this section, the main features of the Lorentz force are taken into account to implement calculated control.

Important to recall that the control force is produced as the result of the direct interaction between Earth's magnetosphere and the satellites charged point of mass. The first step is to calculate the magnetic field vector for the current position of the satellite, according to the equation that is responsible to calculate the Lorentz

force and the satellite velocity vector. Since the Lorentz force direction vector is defined and the control source is the charge of the satellite (a scalar value), it is now possible to implement the calculated control vector at each time step. In order to implement each component of the calculated control, three different values of the satellite charge should be implemented.

Throughout the explanation of the resultant control relations, it is possible to denote the presence of a k parameters in the functions. The key role of this k parameter is associated with the Lyapunov control convergence velocity. It always represents a positive number, whose value and magnitude may vary depending on the available control source. The Lyapunov controls described above are developed without any restrictions concerning the control system. It is then necessary to consider the possible implementation issues when using the Lorentz force.

$$q_x = \frac{u_x}{L_x},\ q_y = \frac{u_y}{L_y},\ q_z = \frac{u_z}{L_z}.$$

where $\begin{bmatrix} u_x & u_y & u_z \end{bmatrix}$ are the control components enumerated in the previous chapter, and $\begin{bmatrix} L_x & L_y & L_z \end{bmatrix}$ are the Lorentz force vector components along the three reference frame axis. However, the charge of the satellite is a scalar value so there cannot be three distinct charges being applied simultaneously. Thus, the calculated control vector cannot be implemented as it is. So, to calculate the single charging value that is going to be applied it is required to calculate a Lorentz force value that is close to joint magnitude of the three calculated control vectors. In order to implement this idea, the following single charge calculation is proposed

$$q_{mean} = \sqrt{\frac{q_x^2 + q_y^2 + q_z^2}{3}} sign\left(q_x + q_y + q_z\right).$$

In this equation a critical step is taken. After obtaining the three values for the required charges (measured along the axis dictated by the Hill reference frame), the main charging value is calculated. This value, q_{mean} , is calculated as the magnitude of the required force and its direction is defined by the strongest component, or components (through the sign function).

As referred to above in this section, during the calculation of the real charging value, the system's charge limitations shall be accounted for. Thus, consider the device's maximum charge value, that can be produced by the charging device, to be qmax. Then whenever the calculated control exceeds the value of qmax the following step is activated

$$q_{mean} = \begin{cases} q_{\max} sign(q_{mean}), & \text{if } |q_{mean}| \geq q_{\max}, \\ q_{mean}, & \text{if } |q_{mean}| < q_{\max}. \end{cases}$$

This formula represents a stage in the control algorithm, which is activated when the virtual charge value exceeds the limit.

Also the limited charging rate is taken into account in the simulation process. So, while the charging device polarity altercation, the charge cannot vary more than d_{charge} , during the time interval corresponding to $t_n - t_{n-1}$. The following formula is representative of the current value q_{mean} at the time step t_n ,

$$q_{mean}\big|_k = q_{mean}\big|_{k-1} + d_{\text{charge}} sign\left(q_{mean}\big|_k - q_{mean}\big|_{k-1}\right), \quad \text{if } \left|\left(q_{mean}\big|_k - q_{mean}\big|_{k-1}\right)\right| > d_{\text{charge}}.$$

The utilization of such a step is due to the fact that in reality the polar charge changing, i.e., the charge sign (or magnitude) altercation is not an instantaneous process. Therefore this step induces a smoother transition between charging polarization's, providing closer to reality simulation results.

So, the implemented vector of the current Lorentz force acting on the satellite charge is calculated using the following formula

$$\mathbf{F}_L = q_{mean}\left(\mathbf{v} \times \mathbf{B}\right).$$

Thus, this chapter defines the general control algorithm that is used for the relative motion control. Though the control strategies could depend on the number of satellites and on the satellites relations. These aspects are covered in the next section.

3. Numerical study

Consider a set of satellites in low Earth Orbit. In this section a performance of the proposed algorithm for two satellite formation flying case and for swarm relative motion is studied depending on the capabilities of the onboard charging device, required relative trajectory, orbital height and inclination. All the simulation parameters values are listed in Table 1.

Table 1. Simulation parameters

Initial conditions	
Initial relative drift, C_1	rand([-0.5;0.5]) m
Initial relative position constants $C_2 - C_6$	rand([5;5]) m
Satellite parameters	
Mass of the satellites, m	1 kg
Maximum charge, q_{max}	10 μC
Orbital parameters	
Orbit altitude, h	500 km
Orbit inclination, i	51.7^o
Algorithms parameters	
Control gains k_a, k_b	10^{-6}, 10^{-4}
Control gains k_x, k_y, k_z	10^{-6}, 10^{-8}, 10^{-7}
Maximal charge change rate, dq/dt	10^{-7} C/s
Required relative orbit parameters $B_1 - B_4$	[0, 10, 10, 10] m
Second stage algorithm threshold for B_1 and B_3	0.05 m, 2.5 m

The parameters are choose to obtain the best performance of the algorithm considering the convergence and the constants errors. The scheme of the simulation is presented in Fig. 4.

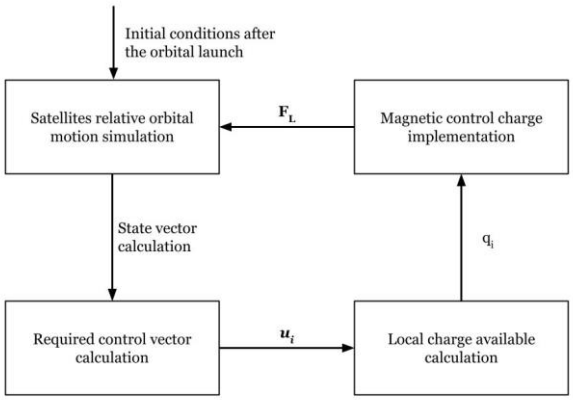

Fig. 4. Scheme of Control Motion Simulation

4.1. Free motion of two satellites

Consider two satellites formation motion with random initial conditions defined above. No control is applied to the satellites. The resulted relative trajectory after simulation is presented in Fig. 5. Since the relative drift is not zero after the launch, relative trajectory is not closed, and the satellites are flying apart. It means that without control it is impossible to obtain close relative trajectories during the whole time of the mission. Even if initially the relative drift is zero, the perturbations lead to gradual drift increase.

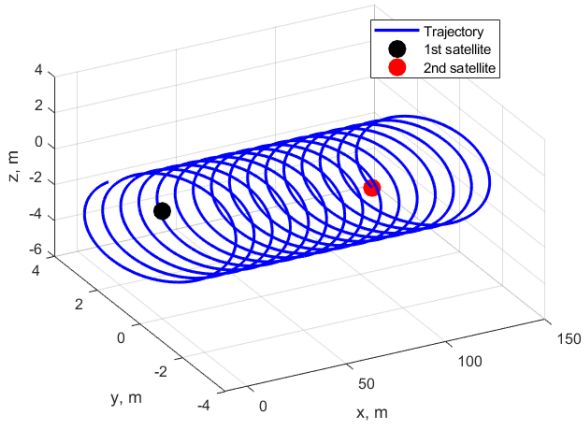

Fig. 5. Relative trajectories of the swarm free motion

4.2. Case of study of one controlled satellite

Consider an application of the proposed control algorithm for the same initial conditions as described for the example of free relative motion. The one of the satellites is considered passively moving along the orbit, the other is controlled using the proposed control algorithm based on Lorenz force. The time of the controlled motion simulation is 5 days. Fig. 6 presents an example of the relative motion. It can be seen that there was an initial drift that was stopped by the first stage of the algorithm. When the parameters relative drift and relative shift B_1 and B_3 entered the vicinity of the required values, the second stage started to change the trajectory amplitudes of the in-plane and out-of-plane. Fig. 7-10 show the values $B_1 - B_4$ of the controlled motion and the required ones. From the plots it can be concluded that the first stage of the algorithm took about 15 hours, when the relative shift and relative drift reached the required values. The second stage was also about 15 hours, during this period the trajectory amplitudes get to the vicinity of the required values. Starting from 30 hours from the simulation beginning the trajectory can be considered as converged to the trajectory with desired shape and size. The control errors caused by the constrains of the value and direction Lorenz force result in errors in trajectory parameters $B_1 - B_4$ during the station keeping of the required trajectory. The maximum deviation of the

relative drift is about 0.05m, and for the relative shift it is about 3m. The errors in the amplitudes B_2 and B_4 are no more than 1 m.

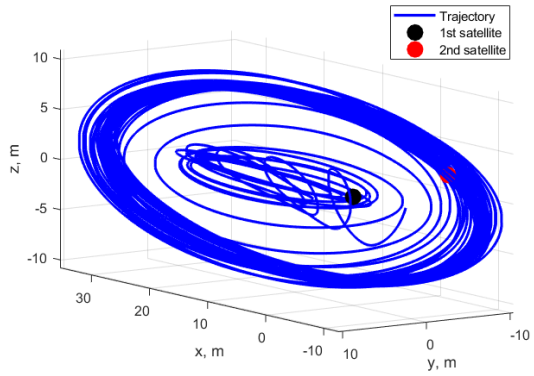

Fig. 6. Relative trajectory under control

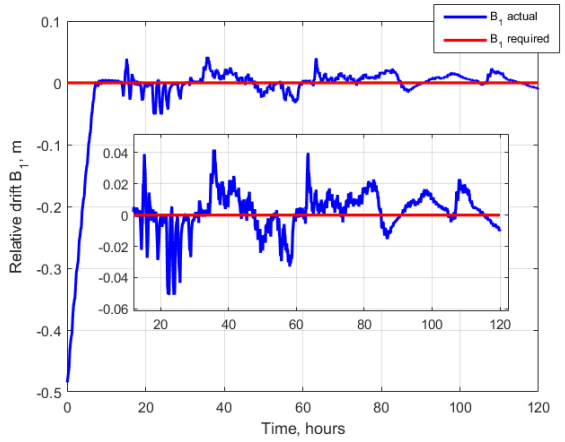

Fig. 7. Relative drift

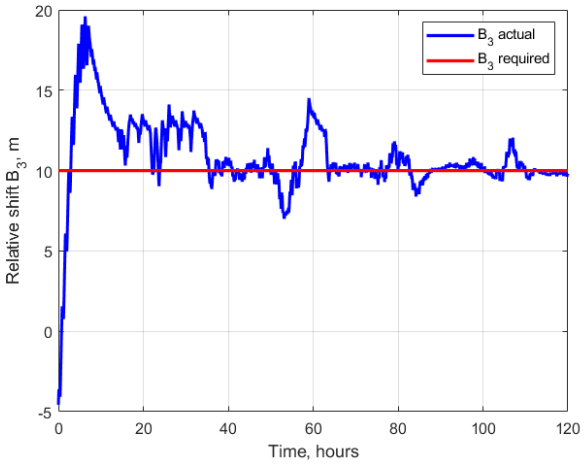

Fig. 8. Relative shift

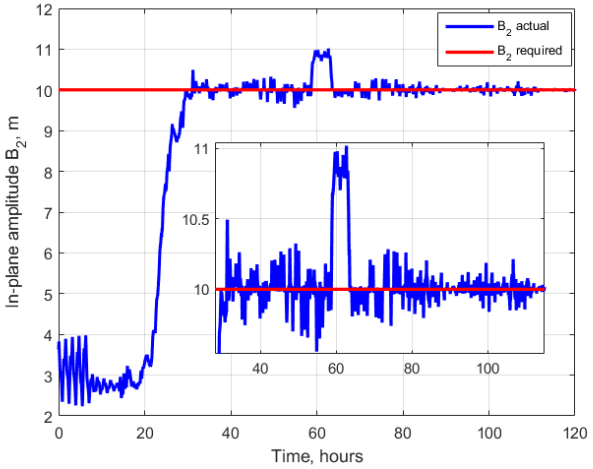

Fig. 9. In-plane amplitude

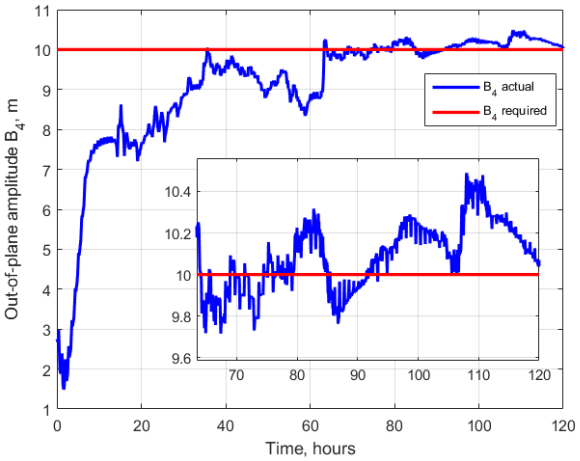

Fig. 10. Out-of-plane amplitude

The value of the implemented charge of the satellite during the control is presented in Fig. 11 and 12. It can be seen that the value of the charge is limited by 10 μC. In zoomed Fig. 12 the continuous change in the charge is demonstrated. The speed of charging is also limited. Even if the calculated value of the charge change the sign it takes time to reach the required value. In such a way the delays in the system are simulated and the limitation of the charging devices are taken into account.

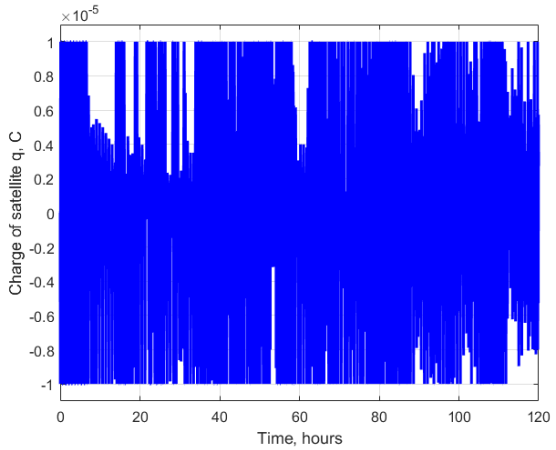

Fig. 11. Satellite charge

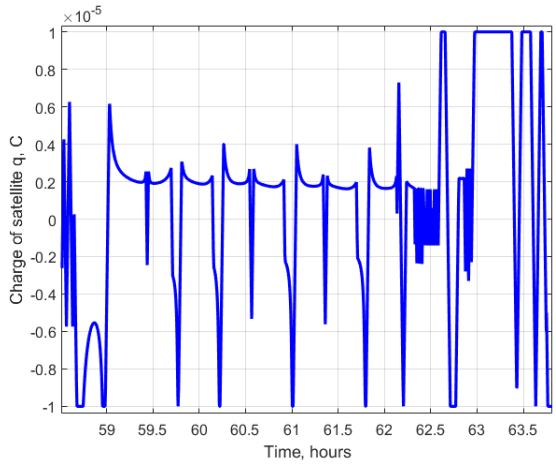

Fig. 12. Satellite charge (zoomed)

The calculated control values according to the Lyapunov-based control algorithm are presented in Fig. 13. The sudden high values for the required control along x direction are caused by transition to the second stage of the algorithm – the deviation of the B_2 amplitude was quite large and it required large control. Though the implemented control through Lorenz force differs significantly from the calculated control as one can see from Fig. 14. The value of the Lorenz force in the along-track direction is of one order smaller than the other components. Nevertheless, it was enough for drift stopping and for convergence to the required shift value. Since the only control parameter in case of Lorenz force is the charge, during implementation the implementation errors are inevitable. The direction of the Lorenz force is determined by the velocity vector and local magnetic field vector. By choosing the charge value only the most significant component of the required control vector is to be partly implemented while the others components are to be implemented with large errors. Though due to magnetic field vector rotation in the LVLH reference frame along the orbit, the errors of implementation are averaging and the trajectory is converging to the required one. From Fig. 14 one can also note a sinusoidal behavior of the peaks of Lorenz forces with period of about 24 hours. It can be explained by the rotational motion of the tilted Earth magnetic dipole that cause the slight change in the possible direction of the Lorenz force.

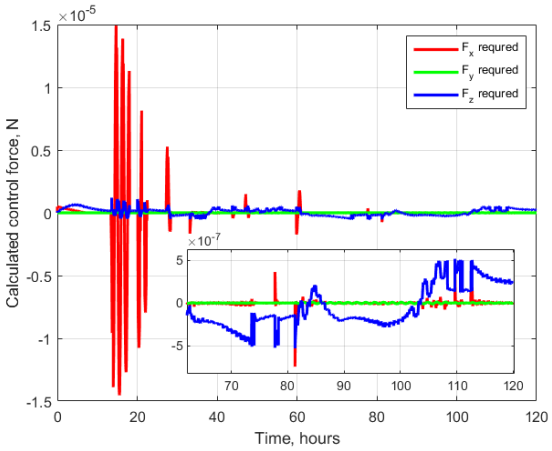

Fig. 13. Calculated control values

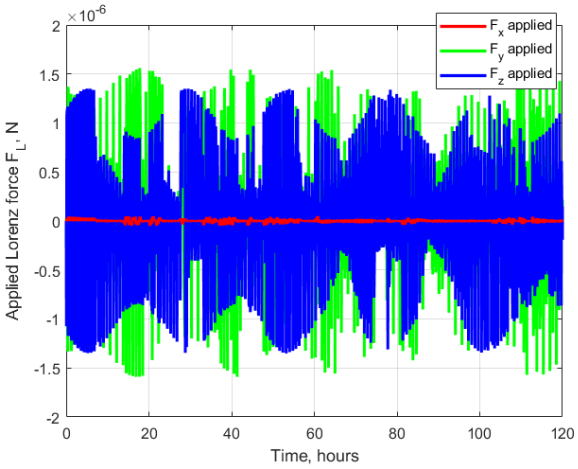

Fig. 14. Applied Lorenz force

The performance of the control algorithm is strongly depend on a set of parameters including the initial conditions. Using Monte-Carlo simulations with random initial conditions described in Table 1 the convergence time and the errors of the obtained trajectory parameters are studied. The convergence time is strongly depend on the initial relative drift B_1 value. For each random maximal initial relative drift where performed 50 numerical simulations. The time of the convergence is defined at a time moment when all the parameters $B_1 - B_4$ are in a certain vicinity of the required values. Fig. 15 demonstrates the box-plots of the results of the simulations. Inside the box are 50 % of the simulations results, below and under the box are 25 %, the red line

is a mean value. One can see that the more the initial drift, the larger the convergence time.

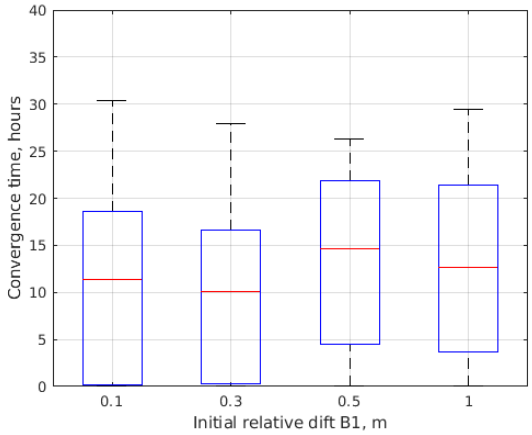

Fig. 15. Convergence time depending on initial drift B_1

It can be concluded that there is no sensible dependence of the errors in the trajectory parameters $B_1 - B_4$ on the initial relative drift value. The errors on the relative drift are no more then 2 m, the errors in B_2 are inside the 0.5 m. The most significant errors are in out-of-plane amplitudes and are about several meters.

Since the control is based on the Lorenz force which is the result of the cross product of the local magnetic field and the velocity it is necessary for the ability to control that the magnetic field should change the direction in inertial reference frame along the orbit. However, if the satellite is in equatorial orbit the geomagnetic field vector is almost constant during the orbital motion. Also, if the satellite is in polar orbit the geomagnetic field vector has components only in orbital plane. These constraints on the geomagnetic field vector direction could influence the control algorithm performance. The Monte-Carlo simulations was performed for the fixed parameters presented in Table 1 and different values of the orbit inclination.

For the equatorial orbit the proposed Lorenz force control is not working as followed from the simulation results. It is caused by the almost fixed geomagnetic field vector along the orbit and as the result the only direction of the Lorenz force. The control algorithm started to achieve the required trajectory beginning from about 30 deg of inclination. The convergence time is less for the polar orbit since the geomagnetic field vector rotates almost in the orbital plane and more control force directions are available along the orbit.

4.3 Cases of satellites swarm

The proposed control can be applied for the formation flying consisting of multiple number of satellites. A swarm of satellites can be used as a spatial distributed measurement system in LEO. Consider a two examples of distributed swarm of nanosatellites controlled using the proposed control algorithm. First example is a formation consisting of *N* satellites with required zero drift and shift relative to the virtual central satellite but different size of the in-plane amplitude. Such a configuration could be useful for construction of the spatial measurement system in space. Second example is a train formation when all the satellite are distributed with the same relative distance in the along-track direction in the orbit. This type of formation is required for Earth-remote sensing problems.

Nested ellipses

Consider a formation flying consisting of 5 satellites. The number of satellites could be larger and the algorithm performance will be the same, though the resulting relative trajectory will be difficult to present. That is why in the case of study only 5 satellites are considered. The initial conditions are the same as in Table 1 except for the required trajectory constants. The required drift and shift is zero for all the satellites $B_1 = 0$, $B_3 = 0$. The out-of plane amplitude is also constant and $B_4 = 10\,\text{m}$. In order to construct the spatially distributed system the required in-plane amplitudes differs by 10m for each satellite. So, after the convergence the satellite trajectories are along the nested ellipses of different size. Fig. 16 shows the example of the relative trajectories of 5 satellites during the 120 hours of simulation, and Fig. 17 presents the resulting trajectories after convergence. As one can see the algorithm is successfully achieved the trajectory of the required size of the ellipses nested inside each other. Fig. 18 and 19 presents the relative drift and shift which are in the vicinity of the required zero value. Fig. 20 shows the convergence of the in-plane amplitudes to the required values. The larger the amplitude the longer it takes to achieve its vicinity. For the 5th satellite it took almost 100 hours to get to the required value of 40 m. The errors in out-of-plane amplitudes are up to 4 m after convergence as one can see in Fig. 21.

In the presented example the control was implemented using centralized approach when all the satellites are follow the motion of the chief satellite, in this case it is the first satellite that is in the center of the nested ellipses. Since the phase of the satellites are not controllable the position of the satellites on the ellipses are random and the planes of the ellipses do not coincide.

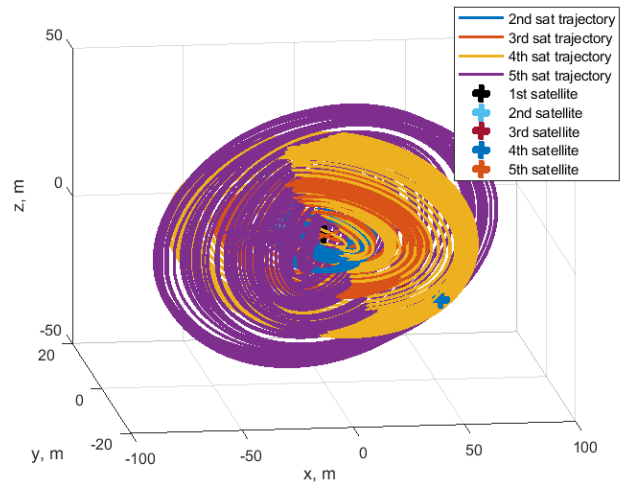

Fig. 16. Relative trajectories

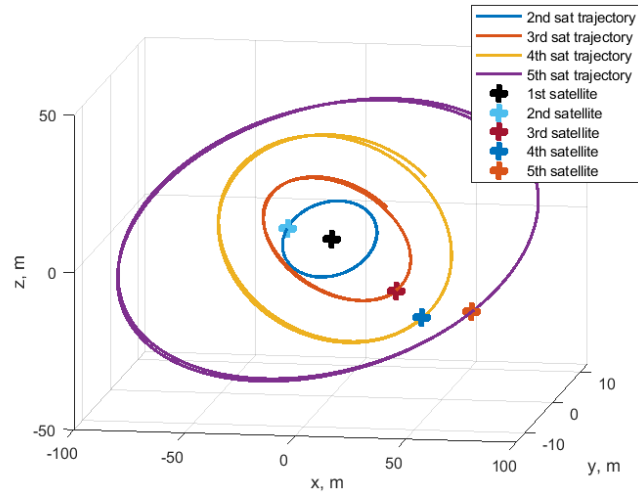

Fig. 17. Relative trajectories during the last 2 hours of simulation

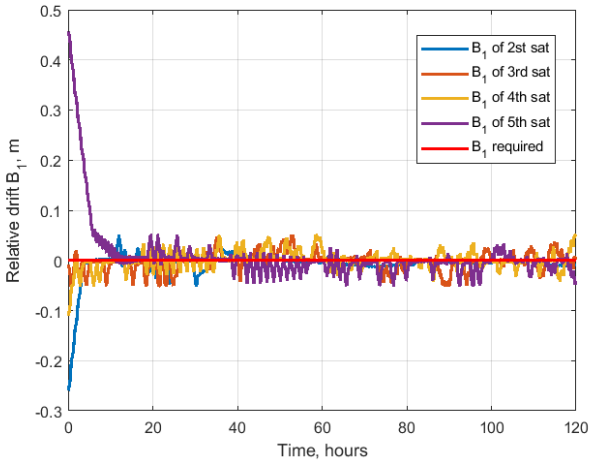

Fig. 18. Relative drift

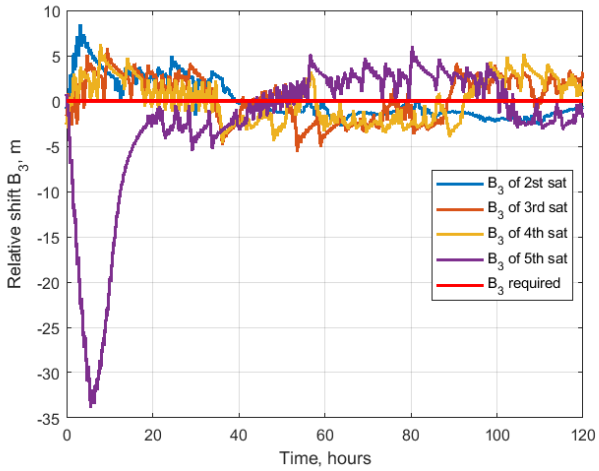

Fig. 19. Relative shift

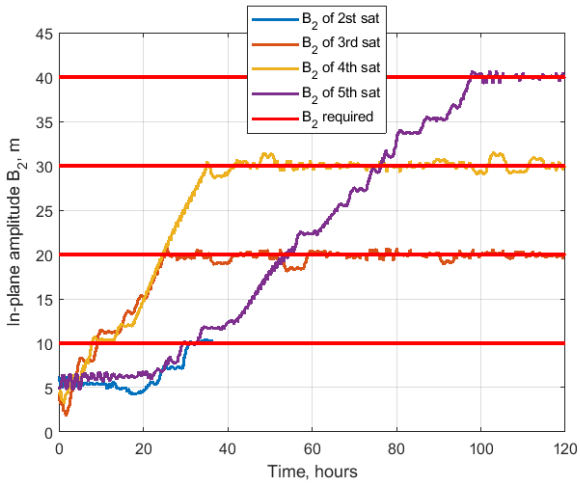

Fig. 20. In-plane amplitude

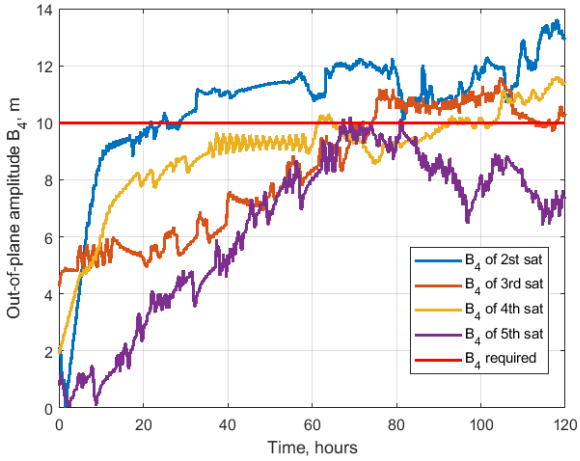

Fig. 21. Out-of-plane amplitude

Train formation

The train formation is used when the uniformly distributed measurements along the same orbit are required for the mission. To achieve such a configuration using the proposed control law the required shift values B_3 should be different and the other parameters B_1, B_2, B_4 should tend to zero. Consider a formation consisting of 5 satellites, all the simulation parameters are the same as for the previous example. In this case the control can be implemented using decentralized approach. Each satellite tries to achieve the required value B_3 of the shift relative to the neighbour satellite with smallest positive value of B_3. Fig. 22 shows the example of the relative trajectories of 5 satellites during the 120 hours of simulation, and Fig. 23 presents the resulting trajectories after convergence. As one can see after a time all the satellites are lined up in along-track direction with separation of 10 m. The out-of-plane amplitudes are of about of 5 m in the end of simulation, and in-plane amplitudes are all around zero except for the second satellite which value of about 0.8 m.

Fig. 24-27 presents the values of the parameters $B_1 - B_4$. The relative drift is close to zero value. But the relative shifts are all at the required values with 10 m of difference. The train configuration the amplitudes should converge to a zero. The in-plane amplitudes are almost all converged to zero after 160 hours of simulation, but the out-of-plane convergence is even slower. After 160 hours of simulation there is the error of several meters. Fig. 28 demonstrates the charges of the satellites. All the values do not exceed the maximum value and after the convergence the values rarely achieve this constraint.

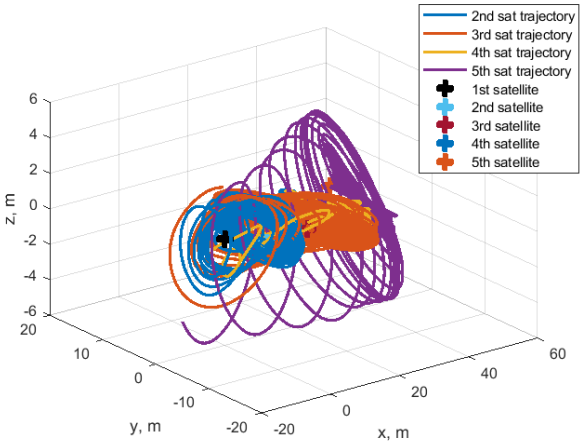

Fig. 22. Relative trajectories

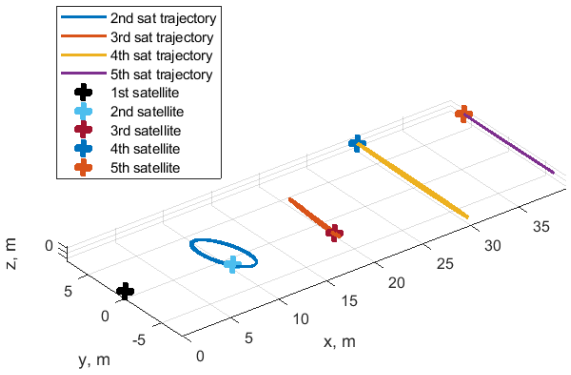

Fig. 23. Relative trajectories during the last 2 hours of simulation

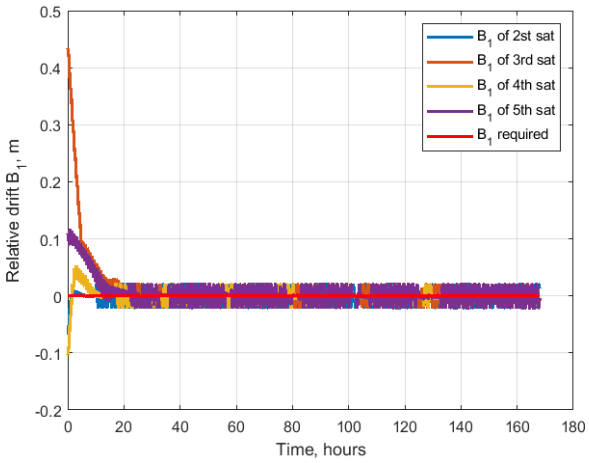

Fig. 24. Relative drift

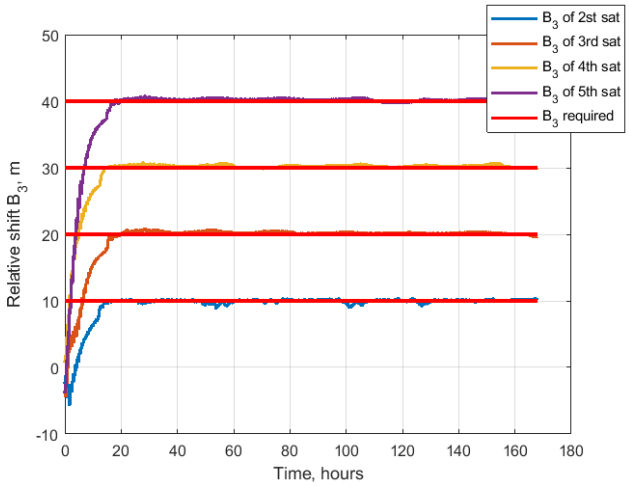

Fig. 25. Relative shift

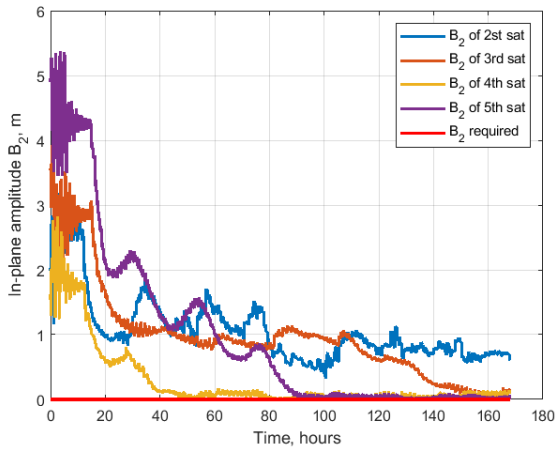

Fig. 26. In-plane amplitude

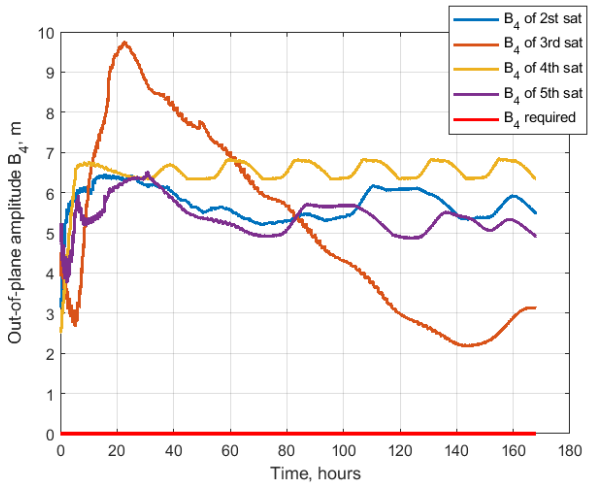

Fig. 27. Out-of-plane amplitude

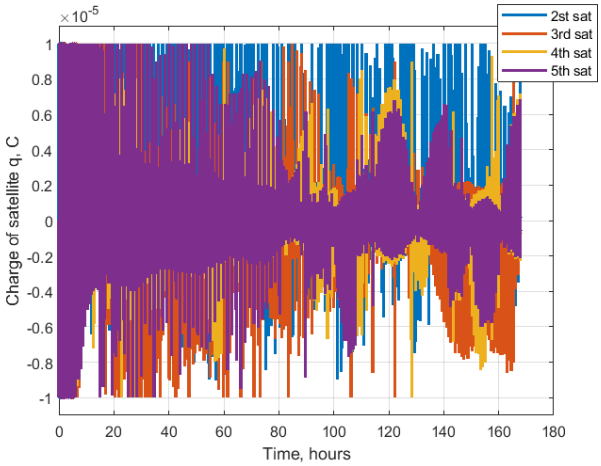

Fig. 28. Charges of the satellites

Thus, the examples of the proposed algorithm application for the construction and maintenance of the two configuration consisting of multiple satellites demonstrate the performance of the algorithm. All the trajectories converged to the required ones with final error of several meters.

5. Conclusions

A control algorithm based on the Lorenz force application is developed for the problems of the construction and maintenance of the small satellites formation flying relative motion. For application of the Lorenz force the onboard charging device capable to provide the required charge of satellite is considered. Since the Lorenz force direction is limited along the orbit and it is determined by the local geomagnetic filed and orbital velocity, only 4 of 6 elements of state vector is controllable. In terms of relative trajectory parameters the proposed Lyapunov-based control is aimed to achieve the required relative drift, relative shift and in-plane and out-of-plane amplitudes. The phases of the in-plane and out-of-plane are considered as uncontrollable. Thus, the required relative configuration, size and shape can be achieved by the proposed control. The numerical study showed that the best algorithm performance could be achieved at near polar orbit. The initial conditions and the maximum possible charge are affect the convergence time as well as the trajectory errors after the convergence. The errors in out-of-plane amplitude is the worst among the errors of the other parameters and could exceed several meters. The results of the application of the proposed algorithm is demonstrated in three cases: the case of one controlled satellite in two satellite formation flying, the case of the two controlled satellites and the two examples of multiple satellites formation flying in nested ellipses and train configurations. In all study cases the control algorithm successfully achieved the required trajectories with final errors of several meters. The proposed Lorenz force based control is perspective for the application onboard the small satellites since it does not require any fuel consumption.

Acknowledgements

The work was partially supported by Project INFANTE – Satellite for marine applications and communications based on constellations, funded by the Portuguese Program COMPETE2020, PORTUGAL2020, and co-funded by the European Structural and Investment Funds. Also it is partially suported by Portuguese Foundation for Science and Technologies via Centre for Mechanical and Aerospace Science and Technologies, C-MAST, POCI-01-0145-FEDER-007718.

References

1. Peck, M.A. Prospects and challenges for lorentz-augmented orbits. *Collect. Tech. Pap. - AIAA Guid. Navig. Control Conf.* **2005**, *3*, 1631–1646, doi:10.2514/6.2005-5995.
2. Schaffer, L.; Burns, J.A. Charged dust in planetary magnetospheres: Hamiltonian dynamics and numerical simulations for highly charged grains. *J. Geophys. Res. Sp. Phys.* **1994**, *99*, 17211–17223, doi:10.1029/94JA01231.
3. Saaj, C.M.; Lappas, V.; Richie, D.; Peck, M.; Streetman, B.; Schaub, H.; Izzo, D. ELECTROSTATIC FORCES FOR SATELLITE SWARM NAVIGATION AND RECONFIGURATION Final Report.
4. Kong, E.M.C.; Kwon, D.W.; Schweighart, S.A.; Elias, L.M.; Sedwick, R.J.; Miller, D.W. Electromagnetic formation flight for multisatellite arrays. *J. Spacecr. Rockets* **2004**, *41*, 659–666, doi:10.2514/1.2172.
5. Kwon, D.W. Propellantless formation flight applications using electromagnetic satellite formations. *Acta Astronaut.* **2010**, *67*, 1189–1201, doi:10.1016/j.actaastro.2010.06.042.
6. Huang, X.; Yan, Y.; Zhou, Y. Optimal spacecraft formation establishment and reconfiguration propelled by the geomagnetic Lorentz force. *Adv. Sp. Res.* **2014**, *54*, 2318–2335, doi:10.1016/j.asr.2014.08.010.
7. Abdel-Aziz, Y.A.; Shoaib, M. Attitude dynamics and control of spacecraft using geomagnetic Lorentz force. *Res. Astron. Astrophys.* **2014**, *15*, 127–144, doi:10.1088/1674-4527/15/1/012.
8. Peng, C.; Gao, Y. Lorentz-force-perturbed orbits with application to J2-invariant formation. *Acta Astronaut.* **2012**, *77*, 12–28, doi:10.1016/J.ACTAASTRO.2012.03.002.
9. Yamakawa, H.; Bando, M.; Yano, K.; Tsujii, S. Spacecraft relative dynamics under the influence of geomagnetic lorentz force. *AIAA/AAS Astrodyn. Spec. Conf. 2010* **2010**, doi:10.2514/6.2010-8128.
10. Tsujii, S.; Bando, M.; Yamakawa, H. Spacecraft Formation Flying Dynamics and Control Using the Geomagnetic Lorentz Force. *J. Guid. Control. Dyn.* **2013**, *36*, 136–148, doi:10.2514/1.57060.
11. Schaub, H.; Junkins, J.L. Analytical Mechanics of Space Systems, Fourth Edition. *Anal. Mech. Sp. Syst. Fourth Ed.* **2018**, doi:10.2514/4.105210.
12. Hill, G.W. Researches in Lunar Theory. *Am. J. Math.* **1878**, *1*, 5–26.
13. Mashtakov, Y.; Ovchinnikov, M.; Petrova, T.; Tkachev, S. Two-satellite formation flying control by cell-structured solar sail. *Acta Astronaut.* **2020**, *170*, 592–600, doi:10.1016/j.actaastro.2020.02.024.
14. Huang, X.; Yan, Y.; Zhou, Y. Optimal Lorentz-augmented spacecraft formation flying in elliptic orbits. *Acta Astronaut.* **2015**, *111*, 37–47, doi:10.1016/j.actaastro.2015.02.012.
15. Finlay, C.C. Models of the Main Geomagnetic Field Based on Multi-satellite Magnetic Data and Gradients—Techniques and Latest Results from the Swarm Mission. *Ionos. Multi-spacecr. Anal. Tools* **2020**, 255–284, doi:10.1007/978-3-030-26732-2_12.
16. Merkin, D.R. *Introduction to the Theory of Stability*; 1997;